Chapter 22
Nonlinear Systems

Nonlinear problems [261, 262] *are of interest to physicists, mathematicians and also engineers. Nonlinear equations are difficult to solve and give rise to interesting phenomena like indeterministic behavior, multistability or formation of patterns in time and space. In the following we discuss recurrence relations like an iterated function* [263]

$$x_{n+1} = f(x_n) \tag{22.1}$$

systems of ordinary differential equations like population dynamics models [264–266]

$$\begin{aligned} \dot{x}(t) &= f(x, y) \\ \dot{y}(t) &= g(x, y) \end{aligned} \tag{22.2}$$

or partial differential equations like the reaction diffusion equation [265, 267, 268]

$$\frac{\partial}{\partial t} c(x,t) = D \frac{\partial^2}{\partial x^2} c(x,t) + f(c) \tag{22.3}$$

where f and g are nonlinear in the mathematical sense.[1] *We discuss fixed points of the logistic mapping and analyze their stability. A bifurcation diagram visualizes the appearance of period doubling and chaotic behavior as a function of a control parameter. The Ljapunov exponent helps to distinguish stable fixed points and periods from chaotic regions. For continuous-time models, the iterated function is replaced by a system of differential equations. For stable equilibria all eigenvalues of the Jacobian matrix must have a negative real part. We discuss the Lotka–Volterra model, which is the simplest model of predator-prey interactions and the Holling-Tanner model, which incorporates functional response. Finally we allow for spatial inhomogeneity and include diffusive terms to obtain reaction-diffusion systems, which show the*

[1] *Linear functions are additive $f(x+y) = f(x) + f(y)$ and homogeneous $f(\alpha x) = \alpha f(x)$.*

P.O.J. Scherer, *Computational Physics*, Graduate Texts in Physics,
DOI 10.1007/978-3-319-61088-7_22

phenomena of traveling waves and pattern formation. Computer experiments study orbits and bifurcation diagram of the logistic map, periodic oscillations of the Lotka–Volterra model, oscillations and limit cycles of the Holling-Tanner model and finally pattern formation in the diffusive Lotka–Volterra model.

22.1 Iterated Functions

Starting from an initial value x_0 a function f is iterated repeatedly

$$\begin{aligned} x_1 &= f(x_0) \\ x_2 &= f(x_1) \\ &\vdots \\ x_{i+1} &= f(x_i). \end{aligned} \tag{22.4}$$

The sequence of function values $x_0, x_1 \cdots$ is called the orbit of x_0. It can be visualized in a 2-dimensional plot by connecting the points

$$(x_0, x_1) \to (x_1, x_1) \to (x_1, x_2) \to (x_2, x_2) \cdots \to (x_i, x_{i+1}) \to (x_{i+1}, x_{i+1})$$

by straight lines (Fig. 22.1).

22.1.1 Fixed Points and Stability

If the equation

$$x^* = f(x^*) \tag{22.5}$$

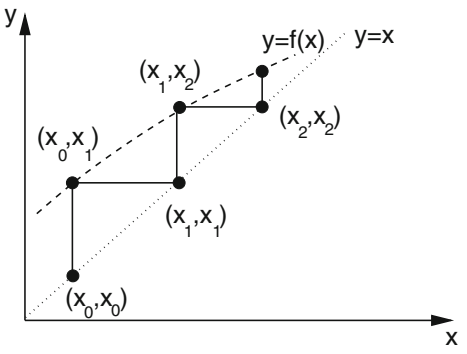

Fig. 22.1 (Orbit of an iterated function) The sequence of points $(x_i, x_{i+1}), (x_{i+1}, x_{i+1})$ is plotted together with the curves $y = f(x)$ (*dashed*) and $y = x$ (*dotted*)

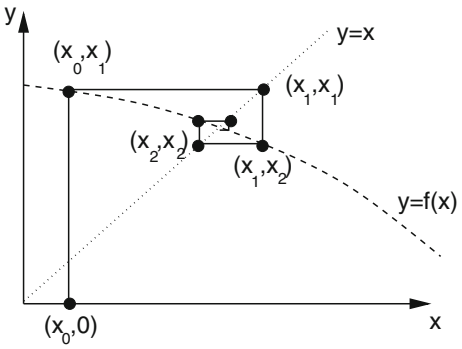

Fig. 22.2 (Attractive fixed point) The orbit of an attractive fixed point converges to the intersection of the curves $y = x$ and $y = f(x)$

has solutions x^*, then these are called fixed points. Consider a point in the vicinity of a fixed point

$$x = x^* + \varepsilon_0 \tag{22.6}$$

and make a Taylor series expansion

$$f(x) = f(x^* + \varepsilon_0) = f(x^*) + \varepsilon_0 f'(x^*) + \cdots = x^* + \varepsilon_1 + \cdots \tag{22.7}$$

with the notation

$$\varepsilon_1 = \varepsilon_0 f'(x^*). \tag{22.8}$$

Repeated iteration gives[2]

$$\begin{aligned} f^{(2)}(x) = f(f(x)) = f(x^* + \varepsilon_1) + \cdots = x^* + \varepsilon_1 f'(x^*) = x^* + \varepsilon_2 \\ \vdots \\ f^{(n)}(x^*) = x^* + \varepsilon_n \end{aligned} \tag{22.9}$$

with the sequence of deviations

$$\varepsilon_n = f'(x^*)\varepsilon_{n-1} = \cdots = \left(f'(x^*)\right)^n \varepsilon_0.$$

The orbit moves away from the fixed point for arbitrarily small ε_0 if $|f'(x^*)| > 1$ whereas the fixed point is attractive for $|f'(x^*)| < 1$ (Fig. 22.2).

Higher order fixed points are defined by iterating $f(x)$ several times. A fixed point of order n simultaneously solves

[2]Here and in the following $f^{(n)}$ denotes an iterated function, not a derivative.

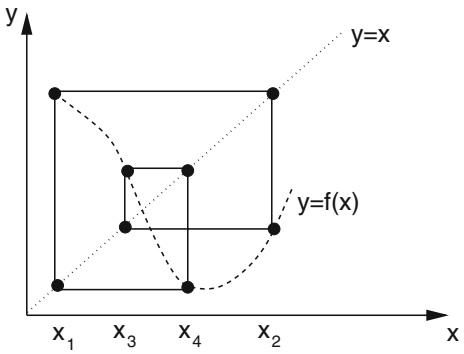

Fig. 22.3 (Periodic orbit) The orbit of an attractive fourth order fixed point cycles through the values $x_1 = f(x_4), x_2 = f(x_1), x_3 = f(x_2), x_4 = f(x_3)$

$$\begin{aligned} f(x^*) &\neq x^* \\ f^{(2)}(x^*) &\neq x^* \\ f^{(n-1)}(x^*) &\neq x^* \\ f^{(n)}(x^*) &= x^*. \end{aligned} \tag{22.10}$$

The iterated function values cycle periodically (Fig. 22.3) through

$$x^* \to f(x^*) \to f^{(2)}(x^*) \cdots f^{(n-1)}(x^*).$$

This period is attractive if

$$|f'(x^*)\, f'(f(x^*))\, f'(f^{(2)}(x^*)) \cdots f'(f^{(n-1)}(x^*))| < 1.$$

22.1.2 The Ljapunov-Exponent

Consider two neighboring orbits with initial values x_0 and $x_0 + \varepsilon_0$. After n iterations the distance is

$$|f(f(\cdots f(x_0))) - f(f(\cdots f(x_0 + \varepsilon_0)))| = |\varepsilon_0| e^{\lambda n} \tag{22.11}$$

with the so called Ljapunov-exponent [269] λ which is useful to characterize the orbit. The Ljapunov-exponent can be determined from

$$\lambda = \lim_{n\to\infty} \frac{1}{n} \ln\left(\frac{|f^{(n)}(x_0 + \varepsilon_0) - f^{(n)}(x_0)|}{|\varepsilon_0|}\right) \tag{22.12}$$

or numerically easier with the approximation

$$|f(x_0+\varepsilon_0)-f(x_0)| = |\varepsilon_0||f'(x_0)|$$

$$\begin{aligned}|f(f(x_0+\varepsilon_0))-f(f(x_0))| &= |(f(x_0+\varepsilon_0)-f(x_0))||f'(x_0+\varepsilon_0)| \\ &= |\varepsilon_0||f'(x_0)||f'(x_0+\varepsilon_0)|\end{aligned} \tag{22.13}$$

$$|f^{(n)}(x_0+\varepsilon_0)-f^{(n)}(x_0)| = |\varepsilon_0||f'(x_0)||f'(x_1)|\cdots|f'(x_{n-1})| \tag{22.14}$$

from

$$\lambda = \lim_{n\to\infty}\frac{1}{n}\sum_{i=0}^{n-1}\ln|f'(x_i)|. \tag{22.15}$$

For a stable fixed point

$$\lambda \to \ln|f'(x^*)| < 0 \tag{22.16}$$

and for an attractive period

$$\lambda \to \ln|f'(x^*)\, f'(f(x^*)\cdots f'(f^{(n-1)}(x^*))| < 0. \tag{22.17}$$

Orbits with $\lambda < 0$ are attractive fixed points or periods. If, on the other hand, $\lambda > 0$, the orbit is irregular and very sensitive to the initial conditions, hence is chaotic.

22.1.3 The Logistic Map

A population of animals is observed yearly. The evolution of the population density N is described in terms of the reproduction rate r by the recurrence relation

$$N_{n+1} = r\, N_n \tag{22.18}$$

where N_n is the population density in year number n. If r is constant, an exponential increase or decrease of N results.

The simplest model for the growth of a population which takes into account that the resources are limited is the logistic model by Verhulst [270]. He assumed that the reproduction rate r depends on the population density N in a simple way (Fig. 22.4)

$$r = r_0(1-\frac{N}{K}). \tag{22.19}$$

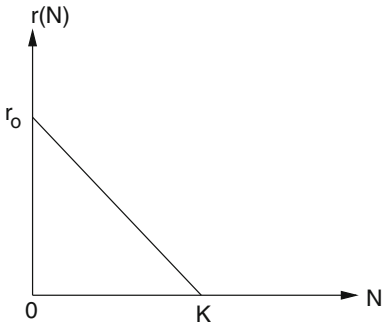

Fig. 22.4 (Reproduction rate of the logistic model) At low densities the growth rate has its maximum value r_0. At larger densities the growth rate declines and reaches $r = 0$ for $N = K$. The parameter K is called carrying capacity

The Verhulst model (22.19) leads to the iterated nonlinear function

$$N_{n+1} = r_0 N_n - \frac{r_0}{K} N_n^2 \tag{22.20}$$

with $r_0 > 0$, $K > 0$. We denote the quotient of population density and carrying capacity by the new variable

$$x_n = \frac{1}{K} N_n \tag{22.21}$$

and obtain an equation with only one parameter, the so called logistic mapping

$$x_{n+1} = \frac{1}{K} N_{n+1} = \frac{1}{K} r_0 N_n \left(1 - \frac{N_n}{K}\right) = r_0 \cdot x_n \cdot (1 - x_n). \tag{22.22}$$

22.1.4 Fixed Points of the Logistic Map

Consider an initial point in the interval

$$0 < x_0 < 1. \tag{22.23}$$

We want to find conditions on r to keep the orbit in this interval. The maximum value of x_{n+1} is found from

$$\frac{\mathrm{d}x_{n+1}}{\mathrm{d}x_n} = r(1 - 2x_n) = 0 \tag{22.24}$$

which gives $x_n = 1/2$ and $\max(x_{n+1}) = r/4$. If $r > 4$ then negative x_n appear after some iterations and the orbit is not bound by a finite interval since

$$\frac{|x_{n+1}|}{|x_n|} = |r|(1 + |x_n|) > 1. \tag{22.25}$$

The fixed point equation

$$x^* = rx^* - rx^{*2} \tag{22.26}$$

always has the trivial solution

$$x^* = 0 \tag{22.27}$$

and a further solution

$$x^* = 1 - \frac{1}{r} \tag{22.28}$$

which is only physically reasonable for $r > 1$, since x should be a positive quantity. For the logistic mapping the derivative is

$$f'(x) = r - 2rx \tag{22.29}$$

which for the first fixed point $x^* = 0$ gives $|f'(0)| = r$. This fixed point is attractive for $0 < r < 1$ and becomes unstable for $r > 1$. For the second fixed point we have $|f'(1 - \frac{1}{r})| = |2 - r|$, which is smaller than one in the interval $1 < r < 3$. For $r < 1$ no such fixed point exists. Finally, for $r_1 = 3$ the first bifurcation appears and higher order fixed points become stable.

Consider the fixed point of the double iteration

$$x^* = r(r(x^* - x^{*^2}) - r^2(x^* - x^{*2})^2). \tag{22.30}$$

All roots of this fourth order equation can be found since we already know two of them. The remaining roots are

$$x^*_{1,2} = \frac{\frac{r+1}{2} \pm \sqrt{r^2 - 2r - 3}}{r}. \tag{22.31}$$

They are real valued if

$$(r - 1)^2 - 4 > 0 \rightarrow r > 3 \quad (\text{or} \quad r < -1). \tag{22.32}$$

For $r > 3$ the orbit oscillates between x_1^* and x_2^* until the next period doubling appears for $r_2 = 1 + \sqrt{6}$. With increasing r more and more bifurcations appear and finally the orbits become chaotic (Fig. 22.5).

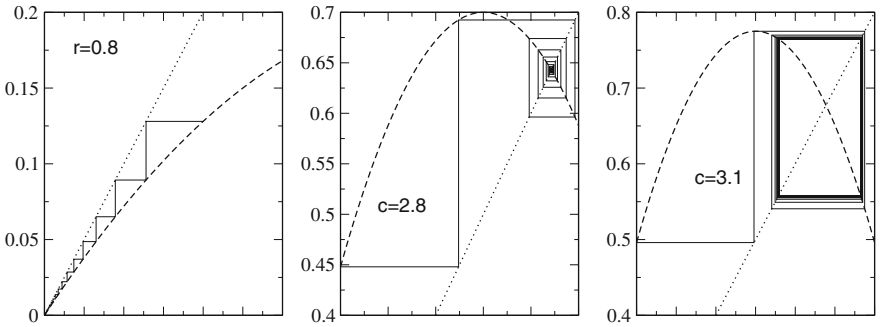

Fig. 22.5 (Orbits of the logistic map) ***Left*** For $0 < r < 1$ the logistic map has the attractive fixed point $x^* = 0$. ***Middle*** In the region $1 < r < 3$ this fixed point becomes unstable and another stable fixed point is at $x^* = 1 - 1/r$. ***Right*** For $3 < r < 1 + \sqrt{6}$ the second order fixed point (22.31) is stable. For larger values of r more and more bifurcations appear

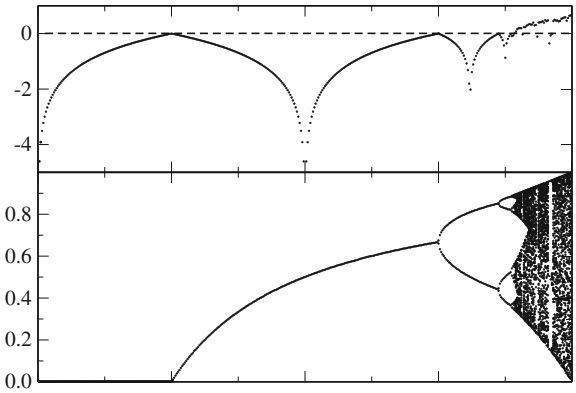

Fig. 22.6 (Bifurcation diagram of the logistic map) For different values of r the function is iterated 1100 times. The first 1000 iterations are dropped to allow the trajectory to approach stable fixed points or periods. The iterated function values $x_{1000} \cdots x_{1100}$ are plotted in a r-x diagram together with the estimate (22.15) of the Ljapunov exponent. The first period doublings appear at $r = 3$ and $r = 1 + \sqrt{6}$. For larger values chaotic behavior is observed and the estimated Ljapunov exponent becomes positive. In some regions motion is regular again with negative Ljapunov exponent

22.1.5 Bifurcation Diagram

The bifurcation diagram visualizes the appearance of period doubling and chaotic behavior as a function of the control parameter r (Fig. 22.6).

22.2 Population Dynamics

If time is treated as a continuous variable, the iterated function has to be replaced by a differential equation

$$\frac{\mathrm{d}N}{\mathrm{d}t} = f(N) \tag{22.33}$$

or, more generally by a system of equations

$$\frac{\mathrm{d}}{\mathrm{d}t}\begin{pmatrix} N_1 \\ N_2 \\ \vdots \\ N_n \end{pmatrix} = \begin{pmatrix} f_1(N_1 \cdots N_n) \\ f_2(N_1 \cdots N_n) \\ \\ f_n(N_1 \cdots N_n) \end{pmatrix}. \tag{22.34}$$

22.2.1 Equilibria and Stability

The role of the fixed points is now taken over by equilibria, which are solutions of

$$0 = \frac{\mathrm{d}N}{\mathrm{d}t} = f(N_{eq}) \tag{22.35}$$

which means roots of $f(N)$. Let us investigate small deviations from equilibrium with the help of a Taylor series expansion. Inserting

$$N = N_{eq} + \xi \tag{22.36}$$

we obtain

$$\frac{\mathrm{d}\xi}{\mathrm{d}t} = f(N_{eq}) + f'(N_{eq})\xi + \cdots \tag{22.37}$$

but since $f(N_{eq}) = 0$, we have approximately

$$\frac{\mathrm{d}\xi}{\mathrm{d}t} = f'(N_{eq})\xi \tag{22.38}$$

with the solution

$$\xi(t) = \xi_0 \exp\left\{f'(N_{eq})t\right\}. \tag{22.39}$$

The equilibrium is only stable if $\mathfrak{Re}\, f'(N_{eq}) < 0$, since then small deviations disappear exponentially. For $\mathfrak{Re}\, f'(N_{eq}) > 0$ deviations will increase, but the

exponential behavior holds only for not too large deviations and saturation may appear. If the derivative $f'(N_{eq})$ has a nonzero imaginary part then oscillations will be superimposed. For a system of equations the equilibrium is defined by

$$\begin{pmatrix} f_1(N_1^{eq} \cdots N_n^{eq}) \\ f_2(N_1^{eq} \cdots N_n^{eq}) \\ \\ f_N(N_1^{eq} \cdots N_n^{eq}) \end{pmatrix} = \begin{pmatrix} 0 \\ 0 \\ \vdots \\ 0 \end{pmatrix} \tag{22.40}$$

and if such an equilibrium exists, linearization gives

$$\begin{pmatrix} N_1 \\ N_2 \\ \vdots \\ N_n \end{pmatrix} = \begin{pmatrix} N_1^{eq} \\ N_2^{eq} \\ \vdots \\ N_n^{eq} \end{pmatrix} + \begin{pmatrix} \xi_1 \\ \xi_2 \\ \vdots \\ \xi_n \end{pmatrix} \tag{22.41}$$

$$\frac{\mathrm{d}}{\mathrm{d}t} \begin{pmatrix} \xi_1 \\ \xi_2 \\ \vdots \\ \xi_N \end{pmatrix} = \begin{pmatrix} \frac{\partial f_1}{\partial N_1} & \frac{\partial f_1}{\partial N_2} & \cdots & \frac{\partial f_1}{\partial N_n} \\ \frac{\partial f_2}{\partial N_1} & \frac{\partial f_2}{\partial N_2} & \cdots & \frac{\partial f_2}{\partial N_n} \\ \vdots & \vdots & \ddots & \vdots \\ \frac{\partial f_n}{\partial N_1} & \frac{\partial f_n}{\partial N_2} & \cdots & \frac{\partial f_n}{\partial N_n} \end{pmatrix} \begin{pmatrix} \xi_1 \\ \xi_2 \\ \vdots \\ \xi_n \end{pmatrix}. \tag{22.42}$$

The equilibrium is stable if all eigenvalues λ_i of the derivative matrix have a negative real part.

22.2.2 The Continuous Logistic Model

The continuous logistic model describes the evolution by the differential equation

$$\frac{dx}{dt} = r_0 x(1-x). \tag{22.43}$$

To find possible equilibria we have to solve

$$x_{eq}(1-x_{eq}) = 0 \tag{22.44}$$

which has the two roots $x_{eq} = 0$ and $x_{eq} = 1$ (Fig. 22.7).

The derivative f' is

$$f'(x) = \frac{\mathrm{d}}{\mathrm{d}x}(r_0 x(1-x)) = r_0(1-2x). \tag{22.45}$$

Since $f'(0) = r_0 > 0$ and $f'(1) = -r_0 < 0$ only the second equilibrium is stable.

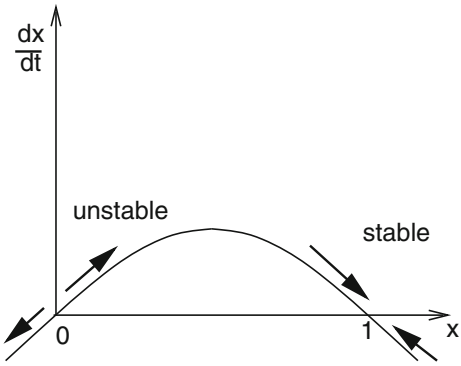

Fig. 22.7 (Equilibria of the logistic model) The equilibrium $x_{eq} = 0$ is unstable since an infinitesimal deviation grows exponentially in time. The equilibrium $x_{eq} = 1$ is stable since initial deviations disappear exponentially

22.3 Lotka–Volterra Model

The model by Lotka [271] and Volterra [272] is the simplest model of predator-prey interactions. It has two variables, the density of prey (H) and the density of predators (P). The overall reproduction rate of each species is given by the difference of the birth rate r and the mortality rate m

$$\frac{\mathrm{d}N}{\mathrm{d}t} = (r - m)N$$

which both may depend on the population densities. The Lotka–Volterra model assumes that the prey mortality depends linearly on the predator density and the predator birth rate is proportional to the prey density

$$m_H = aP \quad r_P = bH \tag{22.46}$$

where a is the predation rate coefficient and b is the reproduction rate of predators per 1 prey eaten. Together we end up with a system of two coupled nonlinear differential equations

$$\frac{\mathrm{d}H}{\mathrm{d}t} = f(H, P) = r_H H - aHP$$

$$\frac{\mathrm{d}P}{\mathrm{d}t} = g(H, P) = bHP - m_P P \tag{22.47}$$

where r_H is the intrinsic rate of prey population increase and m_P the predator mortality rate.

22.3.1 Stability Analysis

To find equilibria we have to solve the system of equations

$$f(H, P) = r_H H - aHP = 0$$

$$g(H, P) = bHP - m_P P = 0. \tag{22.48}$$

The first equation is solved by $H_{eq} = 0$ or by $P_{eq} = r_H/a$. The second equation is solved by $P_{eq} = 0$ or by $H_{eq} = m_P/b$. Hence there are two equilibria, the trivial one

$$P_{eq} = H_{eq} = 0 \tag{22.49}$$

and a nontrivial one

$$P_{eq} = \frac{r_H}{a} \quad H_{eq} = \frac{m_P}{b}. \tag{22.50}$$

Linearization around the zero equilibrium gives

$$\frac{\mathrm{d}H}{\mathrm{d}t} = r_H H + \cdots \quad \frac{\mathrm{d}P}{\mathrm{d}t} = -m_P P + \cdots . \tag{22.51}$$

This equilibrium is unstable since a small prey population will increase exponentially. Now expand around the nontrivial equilibrium:

$$P = P_{eq} + \xi, \quad H = H_{eq} + \eta \tag{22.52}$$

$$\frac{\mathrm{d}\eta}{\mathrm{d}t} = \frac{\partial f}{\partial H}\eta + \frac{\partial f}{\partial P}\xi = (r_H - aP_{eq})\eta - aH_{eq}\xi = -\frac{am_P}{b}\xi \tag{22.53}$$

$$\frac{\mathrm{d}\xi}{\mathrm{d}t} = \frac{\partial g}{\partial H}\eta + \frac{\partial g}{\partial P}\xi = bP_{eq}\eta + (bH_{eq} - m_P)\xi = \frac{br_H}{a}\eta \tag{22.54}$$

or in matrix notation

$$\frac{\mathrm{d}}{\mathrm{d}t}\begin{pmatrix}\eta\\ \xi\end{pmatrix} = \begin{pmatrix}0 & -\frac{am_P}{b}\\ \frac{br_H}{a} & 0\end{pmatrix}\begin{pmatrix}\eta\\ \xi\end{pmatrix}. \tag{22.55}$$

The eigenvalues are purely imaginary

$$\lambda = \pm i\sqrt{m_H r_P} = \pm \mathrm{i}\omega \tag{22.56}$$

and the corresponding eigenvectors are

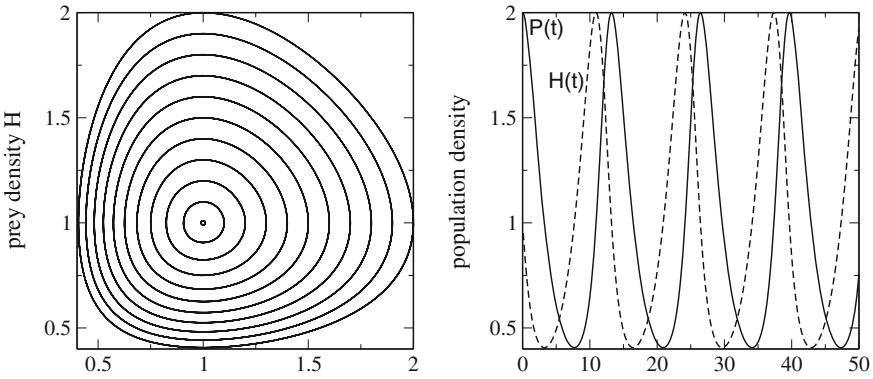

Fig. 22.8 (Lotka Volterra model) The predator and prey population densities show periodic oscillations (***Right***). In the H-P plane the system moves on a closed curve, which becomes an ellipse for small deviations from equilibrium (***Left***)

$$\begin{pmatrix} \mathrm{i}\sqrt{m_H r_p} \\ b r_H / a \end{pmatrix}, \begin{pmatrix} a m_P / b \\ \mathrm{i}\sqrt{m_H r_P} \end{pmatrix}. \tag{22.57}$$

The solution of the linearized equations is then given by

$$\begin{aligned} \xi(t) &= \xi_0 \cos \omega t + \frac{b}{a}\sqrt{\frac{r_P}{m_H}}\eta_0 \sin \omega t \\ \eta(t) &= \eta_0 \cos \omega t - \frac{a}{b}\sqrt{\frac{m_H}{r_P}}\xi_0 \sin \omega t \end{aligned} \tag{22.58}$$

which describes an ellipse in the $\xi - \eta$ plane (Fig. 22.8). The nonlinear equations (22.48) have a first integral

$$r_H \ln P(t) - a\, P(t) - b\, H(t) + m_P \ln H(t) = C \tag{22.59}$$

and therefore the motion in the $H - P$ plane is on a closed curve around the equilibrium which approaches an ellipse for small amplitudes ξ, η.

22.4 Functional Response

Holling [273, 274] studied predation of small mammals on pine sawflies. He suggested a very popular model of functional response. Holling assumed that the predator spends its time on two kinds of activities, searching for prey and prey handling (chasing, killing, eating, digesting). The total time equals the sum of time spent on searching and time spent on handling

$$T = T_{search} + T_{handling}. \tag{22.60}$$

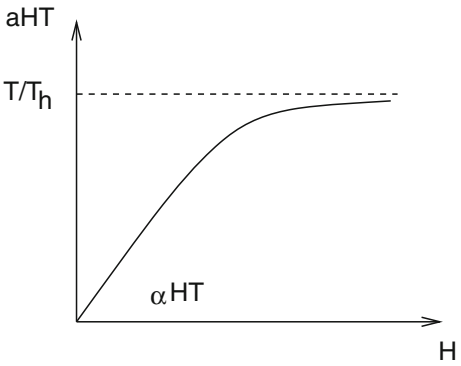

Fig. 22.9 Functional response of Holling's model

Capturing prey is assumed to be a random process. A predator examines an area α per time and captures all prey found there. After spending the time T_{search} the predator examined an area of αT_{search} and captured $H_T = H\alpha T_{search}$ prey. Hence the predation rate is

$$a = \frac{H_T}{HT} = \alpha \frac{T_{search}}{T} = \alpha \frac{1}{1 + T_{handling}/T_{search}}. \tag{22.61}$$

The handling time is assumed to be proportional to the number of prey captured

$$T_{handling} = T_h H \alpha T_{search} \tag{22.62}$$

where T_h is the handling time spent per one prey. The predation rate then is given by

$$a = \frac{\alpha}{1 + \alpha H T_h}. \tag{22.63}$$

At small densities handling time is unimportant and the predation rate is $a_0 = \alpha$ whereas at high prey density handling limits the number of prey captured and the predation rate approaches $a_\infty = \frac{1}{HT_h}$ (Fig. 22.9).

22.4.1 Holling-Tanner Model

We combine the logistic model with Holling's model for the predation rate [273–275]

$$\frac{dH}{dt} = r_H H \left(1 - \frac{H}{K_H}\right) - aHP = r_H H \left(1 - \frac{H}{K_H}\right) - \frac{\alpha}{1 + \alpha H T_h} HP = f(H, P) \tag{22.64}$$

and assume that the carrying capacity of the predator is proportional to the density of prey

$$\frac{dP}{dt} = r_P P\left(1 - \frac{P}{K_P}\right) = r_P P\left(1 - \frac{P}{kH}\right) = g(H, P). \tag{22.65}$$

Obviously there is a trivial equilibrium with $P_{eq} = H_{eq} = 0$. Linearization gives

$$\frac{\mathrm{d}H}{\mathrm{d}t} = r_H H + \cdots \quad \frac{\mathrm{d}P}{\mathrm{d}t} = r_P P + \cdots \tag{22.66}$$

which shows that this equilibrium is unstable. There is another trivial equilibrium with $P_{eq} = 0, \quad H_{eq} = K_H$. After linearization

$$P = \xi + \ldots \quad H = K_H + \eta + \ldots \tag{22.67}$$

we find

$$\frac{\mathrm{d}\eta}{\mathrm{d}t} = r_H(K_H + \eta)(1 - \frac{K_H + \eta}{K_H}) - \frac{\alpha}{1 + \alpha(K_H + \eta)T_h}(K_H + \eta)\xi + \ldots$$

$$= -r_H\eta - \frac{\alpha}{1 + \alpha K_H T_h} K_H \xi + \ldots \tag{22.68}$$

$$\frac{\mathrm{d}\xi}{\mathrm{d}t} = r_P \xi. \tag{22.69}$$

The eigenvalues of the linearized equations

$$\begin{pmatrix} \dot{\eta} \\ \dot{\xi} \end{pmatrix} = \begin{pmatrix} r_H & -\frac{\alpha}{1+\alpha K_H T_h} K_H \\ 0 & r_P \end{pmatrix} \begin{pmatrix} \eta \\ \xi \end{pmatrix} \tag{22.70}$$

are

$$\lambda = \frac{r_H + r_P}{2} \pm \frac{1}{2}\sqrt{(r_H - r_P)^2} = r_H, r_P. \tag{22.71}$$

Let us now look for nontrivial equilibria. The nullclines (Fig. 22.10) are the curves defined by $\frac{dH}{dt} = 0$ and $\frac{dP}{dt} = 0$, hence by

$$P = \frac{r_H}{\alpha}\left(1 - \frac{H}{K_H}\right)(1 + \alpha H T_h) \tag{22.72}$$

$$P = kH. \tag{22.73}$$

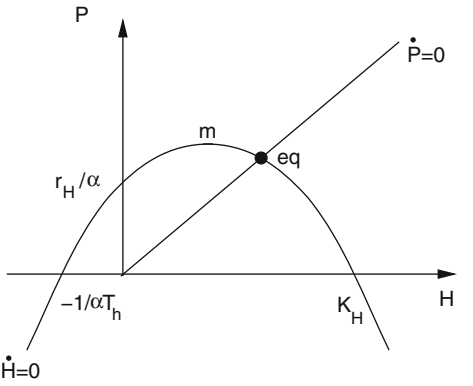

Fig. 22.10 Nullclines of the predator prey model

The H-nullcline is a parabola at

$$H_m = \frac{\alpha T_h - K_H^{-1}}{2\alpha T_h K_H^{-1}} \quad P_m = \frac{(\alpha T_h + K_H^{-1})^2}{4\alpha T_h K_H^{-1}} > 0. \tag{22.74}$$

It intersects the H-axis at $H = K_H$ and $H = -1/\alpha T_h$ and the P-axis at $P = r_H/\alpha$. There is one intersection of the two nullclines at positive values of H and P which corresponds to a nontrivial equilibrium. The equilibrium density H_{eq} is the positive root of

$$r_H \alpha T_h H_{eq}^2 + (r_H + \alpha k K_H - r_H K_H \alpha T_h)\, H_{eq} - r_H K_H = 0. \tag{22.75}$$

It is explicitly given by

$$\begin{aligned} H_{eq} = &-\frac{r_H + \alpha k K_H - r_H K_H \alpha T_h}{2 r_H \alpha T_h} \\ &+ \frac{\sqrt{(r_H + \alpha k K_H - r_H K_H \alpha T_h)^2 + 4 r_H \alpha T_h r_H K_H}}{2 r_H \alpha T_h}. \end{aligned} \tag{22.76}$$

The prey density then follows from

$$P_{eq} = H_{eq} k. \tag{22.77}$$

The matrix of derivatives has the elements

$$\begin{aligned} m_{HP} &= \frac{\partial f}{\partial P} = -\frac{\alpha H_{eq}}{1 + \alpha T_h H_{eq}} \\ m_{HH} &= \frac{\partial f}{\partial H} = r_H \left(1 - 2\frac{H_{eq}}{K_H}\right) - \frac{\alpha k H_{eq}}{1 + \alpha T_h H_{eq}} + \frac{\alpha^2 H_{eq}^2 k T_h}{(1 + \alpha T_h H_{eq})^2} \\ m_{PP} &= \frac{\partial g}{\partial P} = = -r_P \end{aligned}$$

$$m_{PH} = \frac{\partial g}{\partial H} = r_P k \tag{22.78}$$

from which the eigenvalues are calculated as

$$\lambda = \frac{m_{HH} + m_{PP}}{2} \pm \sqrt{\frac{(m_{HH} + m_{PP})^2}{4} - (m_{HH} m_{PP} - m_{HP} m_{PH})}. \tag{22.79}$$

Oscillations appear, if the squareroot is imaginary (Fig. 22.11).

22.5 Reaction-Diffusion Systems

So far we considered spatially homogeneous systems where the density of a population, or the concentration of a chemical agent, depend only on time. If we add spatial inhomogeneity and diffusive motion, new and interesting phenomena like pattern formation or traveling excitations can be observed.

22.5.1 General Properties of Reaction-Diffusion Systems

Reaction-diffusion systems are described by a diffusion equation[3] where the source term depends non-linearly on the concentrations

$$\frac{\partial}{\partial t} \begin{pmatrix} c_1 \\ \vdots \\ c_N \end{pmatrix} = \begin{pmatrix} D_1 & & \\ & \ddots & \\ & & D_N \end{pmatrix} \triangle \begin{pmatrix} c_1 \\ \vdots \\ c_N \end{pmatrix} + \begin{pmatrix} F_1(\{c\}) \\ \vdots \\ F_N(\{c\}) \end{pmatrix}. \tag{22.80}$$

22.5.2 Chemical Reactions

Consider a number of chemical reactions which are described by stoichiometric equations

$$\sum_i \nu_i A_i = 0. \tag{22.81}$$

[3] We consider only the case, that different species diffuse independently and that the diffusion constants do not depend on direction.

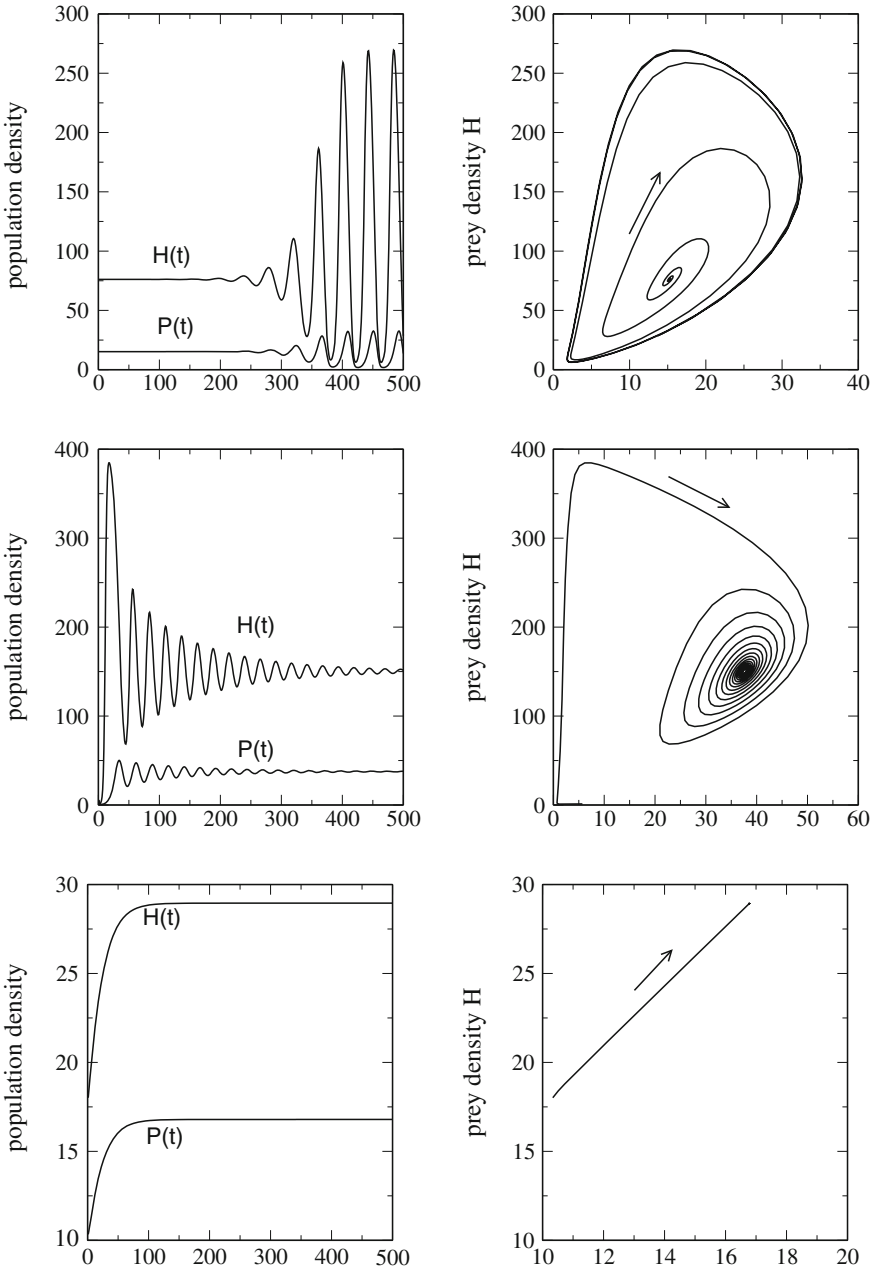

Fig. 22.11 (Holling-Tanner model) ***Top*** evolution from an unstable equilibrium to a limit cycle. ***Middle*** a stable equilibrium is approached with oscillations. ***Bottom*** stable equilibrium without oscillations

The concentration of agent A_i is

$$c_i = c_{i,0} + \nu_i x \tag{22.82}$$

with the reaction variable

$$x = \frac{c_i - c_{i,0}}{\nu_i} \tag{22.83}$$

and the reaction rate

$$r = \frac{\mathrm{d}x}{\mathrm{d}t} = \frac{1}{\nu_i}\frac{\mathrm{d}c_i}{\mathrm{d}t} \tag{22.84}$$

which, in general is a nonlinear function of all concentrations. The total concentration change due to diffusion and reactions is given by

$$\frac{\partial}{\partial t}c_k = D_k \triangle c_k + \sum_j \nu_{kj} r_j = D_k \triangle c_k + F_k(\{c_i\}). \tag{22.85}$$

22.5.3 Diffusive Population Dynamics

Combination of population dynamics (22.2) and diffusive motion gives a similar set of coupled equations for the population densities

$$\frac{\partial}{\partial t}N_k = D_k \triangle N_k + f_k(N_1, N_2, \cdots N_n). \tag{22.86}$$

22.5.4 Stability Analysis

Since a solution of the nonlinear equations is not generally possible we discuss small deviations from an equilibrium solution N_k^{eq}[4] with

$$\frac{\partial}{\partial t}N_k = \triangle N_k = 0. \tag{22.87}$$

Obviously the equilibrium obeys

$$f_k(N_1 \cdots N_n) = 0 \quad k = 1, 2 \cdots n. \tag{22.88}$$

[4] We assume tacitly that such a solution exists.

We linearize the equations by setting

$$N_k = N_k^{eq} + \xi_k \tag{22.89}$$

and expand around the equilibrium

$$\frac{\partial}{\partial t}\begin{pmatrix}\xi_1\\ \xi_2\\ \vdots\\ \xi_n\end{pmatrix} = \begin{pmatrix} D_1 & & \\ & \ddots & \\ & & D_N\end{pmatrix}\begin{pmatrix}\triangle\xi_1\\ \triangle\xi_2\\ \vdots\\ \triangle\xi_n\end{pmatrix} + \begin{pmatrix} \frac{\partial f_1}{\partial N_1} & \frac{\partial f_1}{\partial N_2} & \cdots & \frac{\partial f_1}{\partial N_n}\\ \frac{\partial f_2}{\partial N_1} & \frac{\partial f_2}{\partial N_2} & \cdots & \frac{\partial f_2}{\partial N_n}\\ \vdots & \vdots & \ddots & \vdots\\ \frac{\partial f_n}{\partial N_1} & \frac{\partial f_n}{\partial N_2} & \cdots & \frac{\partial f_n}{\partial N_n}\end{pmatrix}\begin{pmatrix}\xi_1\\ \xi_2\\ \vdots\\ \xi_n\end{pmatrix} + \cdots . \tag{22.90}$$

Plane waves are solutions of the linearized problem.[5] Using the ansatz

$$\xi_j = \xi_{j,0} \mathrm{e}^{\mathrm{i}(\omega t - \mathbf{kx})} \tag{22.91}$$

we obtain

$$i\omega \begin{pmatrix}\xi_1\\ \xi_2\\ \vdots\\ \xi_n\end{pmatrix} = -k^2 D \begin{pmatrix}\xi_1\\ \xi_2\\ \vdots\\ \xi_n\end{pmatrix} + M_0 \begin{pmatrix}\xi_1\\ \xi_2\\ \vdots\\ \xi_n\end{pmatrix} \tag{22.92}$$

where M_0 denotes the matrix of derivatives and D the matrix of diffusion constants. For a stable plane wave solution $\lambda = i\omega$ is an eigenvalue of

$$M_k = M_0 - k^2 D \tag{22.93}$$

with

$$\Re(\lambda) \leq 0. \tag{22.94}$$

If there are purely imaginary eigenvalues for some $\mathbf{k}$ they correspond to stable solutions which are spatially inhomogeneous and lead to formation of certain patterns. Interestingly, diffusion can lead to instabilities even for a system which is stable in the absence of diffusion [276].

[5] Strictly this is true only for an infinite or periodic system.

22.5.5 Lotka Volterra Model with Diffusion

As a simple example we consider again the Lotka Volterra model. Adding diffusive terms we obtain the equations

$$\frac{\partial}{\partial t}\begin{pmatrix} H \\ P \end{pmatrix} = \begin{pmatrix} r_H H - aHP \\ bHP - m_P P \end{pmatrix} + \begin{pmatrix} D_H & \\ & D_P \end{pmatrix} \Delta \begin{pmatrix} H \\ P \end{pmatrix}. \tag{22.95}$$

There are two equilibria

$$H_{eq} = P_{eq} = 0 \tag{22.96}$$

and

$$P_{eq} = \frac{r_H}{a} \quad H_{eq} = \frac{m_P}{b}. \tag{22.97}$$

The Jacobian matrix is

$$M_0 = \frac{\partial}{\partial C} F(C_0) = \begin{pmatrix} r_H - aP_{eq} & -aH_{eq} \\ bP_{eq} & bH_{eq} - m_P \end{pmatrix} \tag{22.98}$$

which gives for the trivial equilibrium

$$M_k = \begin{pmatrix} r_H - D_H k^2 & 0 \\ 0 & -m_P - D_P k^2 \end{pmatrix}. \tag{22.99}$$

One eigenvalue $\lambda_1 = -m_P - D_P k^2$ is negative whereas the second $\lambda_2 = r_H - D_H k^2$ is positive for $k^2 < r_H/D_H$. Hence this equilibrium is unstable against fluctuations with long wavelengths. For the second equilibrium we find:

$$M_k = \begin{pmatrix} -D_H k^2 & -\frac{am_P}{b} \\ \frac{br_H}{a} & -D_P k^2 \end{pmatrix} \tag{22.100}$$

$$\text{tr}\,(M_k) = -(D_H + D_P)k^2$$

$$\det(M_K) = m_P r_H + D_H D_P k^4$$

$$\lambda = -\frac{D_H + D_P}{2} k^2 \pm \frac{1}{2}\sqrt{(D_H - D_P)^2 k^4 - 4m_P r_H}. \tag{22.101}$$

For small k with $k^2 < 2\sqrt{m_P r_H}/|D_H - D_P|$ damped oscillations are expected whereas the system is stable against fluctuations with larger k (Figs. 22.12, 22.13 and 22.14).

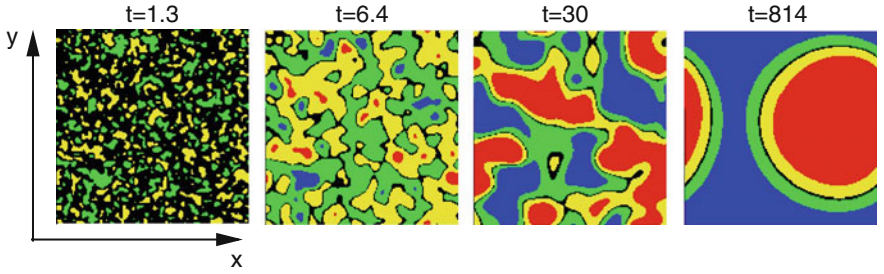

Fig. 22.12 (Lotka–Volterra model with diffusion) The time evolution is calculated for initial random fluctuations. *Colors* indicate the deviation of the predator concentration $P(x, y, t)$ from its average value (*blue*: $\Delta P < -0.1$, *green*: $-0.1 < \Delta P < -0.01$, *black*: $-0.01 < \Delta P < 0.01$, *yellow*: $0.01 < \Delta P < 0.1$, *red*: $\Delta P > 0.1$). Parameters as in Fig. 22.13

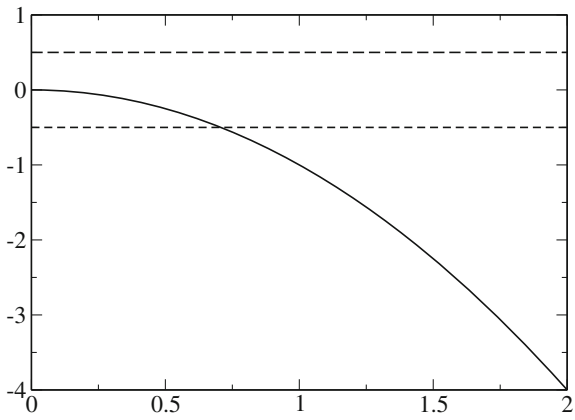

Fig. 22.13 (Dispersion of the diffusive Lotka–Volterra model) Real (*full curve*) and imaginary part (*broken line*) of the eigenvalue λ (22.101) are shown as a function of k. Parameters are $D_H = D_P = 1$, $m_P = r_H = a = b = 0.5$

Problems

Problem 22.1: Orbits of the Iterated Logistic Map

This computer example draws orbits (Fig. 22.5) of the logistic map

$$x_{n+1} = r_0 \cdot x_n \cdot (1 - x_n). \tag{22.102}$$

You can select the initial value x_0 and the variable r.

Problem 22.2: Bifurcation Diagram of the Logistic Map

This computer example generates a bifurcation diagram of the logistic map (Fig. 22.6). You can select the range of r.

Problem 22.3: Lotka–Volterra Model

Equation (22.47) are solved with the improved Euler method (Fig. 22.8). The predictor step uses an explicit Euler step to calculate the values at $t + \Delta t/2$

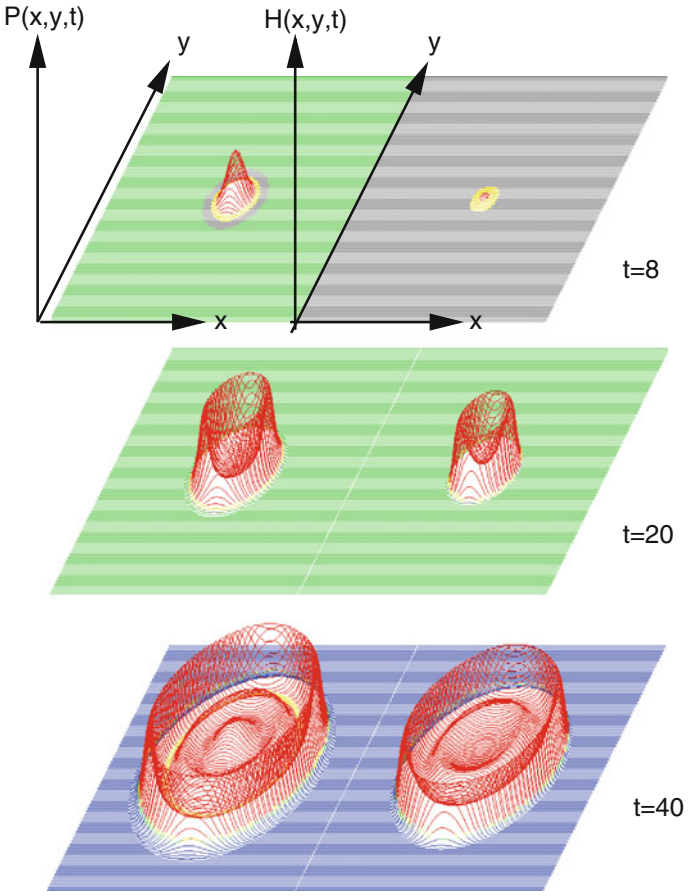

Fig. 22.14 (Traveling waves in the diffusive Lotka–Volterra model) Initially $P(x, y) = P_{eq}$ and $H(x, y)$ is peaked in the center. This leads to oscillations and a sharp wavefront moving away from the excitation. Color code and parameters as in Fig. 22.12

$$H_{pr}(t + \frac{\Delta t}{2}) = H(t) + (r_H H(t) - aH(t)P(t))\,\frac{\Delta t}{2} \tag{22.103}$$

$$P_{pr}(t + \frac{\Delta t}{2}) = P(t) + \left(bH(t)P(t) - m_p P(t)\right)\frac{\Delta t}{2} \tag{22.104}$$

and the corrector step advances time by Δt

$$H(t + \Delta t) = H(t) + \left(r_H H_{pr}(t + \frac{\Delta t}{2}) - aH_{pr}(t + \frac{\Delta t}{2})P_{pr}(t + \frac{\Delta t}{2})\right)\Delta t \tag{22.105}$$

$$P(t+\Delta t) = P(t) + \left(bH_{pr}(t+\frac{\Delta t}{2}) P_{pr}(t+\frac{\Delta t}{2}) - m_p P_{pr}(t+\frac{\Delta t}{2}) \right) \Delta t. \tag{22.106}$$

Problem 22.4: Holling-Tanner Model

The equations of the Holling-Tanner model (22.64), (22.65) are solved with the improved Euler method (see Fig. 22.11). The predictor step uses an explicit Euler step to calculate the values at $t + \Delta t/2$:

$$H_{pr}(t+\frac{\Delta t}{2}) = H(t) + f(H(t), P(t))\frac{\Delta t}{2} \tag{22.107}$$

$$P_{pr}(t+\frac{\Delta t}{2}) = P(t) + g(H(t), P(t))\frac{\Delta t}{2} \tag{22.108}$$

and the corrector step advances time by Δt:

$$H(t+\Delta t) = H(t) + f(H_{pr}(t+\frac{\Delta t}{2}), P_{pr}(t+\frac{\Delta t}{2}))\Delta t \tag{22.109}$$

$$P(t+\Delta t) = P(t) + g(H_{pr}(t+\frac{\Delta t}{2}), P_{pr}(t+\frac{\Delta t}{2}))\Delta t. \tag{22.110}$$

Problem 22.5: Diffusive Lotka–Volterra Model

The Lotka–Volterra model with diffusion (22.95) is solved in 2 dimensions with an implicit method (21.2.2) for the diffusive motion (Figs. 22.12 and 22.14). The split operator approximation (21.3) is used to treat diffusion in x and y direction independently. The equations

$$\begin{pmatrix} H(t+\Delta t) \\ P(t+\Delta t) \end{pmatrix} = \begin{pmatrix} A^{-1}H(t) \\ A^{-1}P(t) \end{pmatrix} + \begin{pmatrix} A^{-1}f(H(t), P(t))\Delta t \\ A^{-1}g(H(t), P(t))\Delta t \end{pmatrix}$$

$$\approx \begin{pmatrix} A_x^{-1}A_y^{-1}\left[H(t) + f(H(t), P(t))\Delta t\right] \\ A_x^{-1}A_y^{-1}\left[P(t) + g(H(t), P(t))\Delta t\right] \end{pmatrix} \tag{22.111}$$

are equivalent to the following systems of linear equations with tridiagonal matrix (5.3):

$$A_y U = H(t) + f(H(t), P(t))\Delta t \tag{22.112}$$

$$U = A_x H(t+\Delta t) \tag{22.113}$$

$$A_y V = P(t) + g(H(t), P(t))\Delta t \tag{22.114}$$

$$V = A_x P(t+\Delta t). \tag{22.115}$$

Periodic boundary conditions are implemented with the method described in Sect. 5.4.